ACS OMEGA

Article

http://pubs.acs.org/journal/acsodf

Effects of Nanosecond Pulsed Electric Field on Intracellular NADH Autofluorescence: A Comparison between Normal and Cancer Cells

Kamlesh Awasthi,[†] Takakazu Nakabayashi,[‡] Liming Li,[§] and Nobuhiro Ohta*[,†]

[†]Department of Applied Chemistry and Institute of Molecular Science, National Chiao Tung University, 1001, Ta-Hsueh Road, Hsinchu 30010, Taiwan

[‡]Graduate School of Pharmaceutical Sciences, Tohoku University, Aoba-ku, Sendai 980-8578, Japan

[§]Department of Bio- and Material Photonics, Chitose Institute of Science and Technology, Chitose 066-8655, Japan

Supporting Information

ABSTRACT: Intracellular fluorescence lifetime and intensity images of the endogenous fluorophore of nicotinamide adenine dinucleotide (NADH) have been observed before and after application of nanosecond pulsed electric field (nsPEF) in normal and cancer cells, that is, in Wistar-King-Aptekman rat fetus fibroblast (WFB) cells and W31 cells, which are the malignant transformed cells from WFB. The application of nsPEF induces a change both in intensity and lifetime of NADH, indicating that the intracellular function is affected by application of nsPEF in both normal and cancer cells. The application of nsPEF induces an increase in the fluorescence lifetime of NADH and a morphological change, which is attributed to the induction of apoptosis by nsPEF. The field effect on the intensity and lifetime clearly depends on the pulse width, and magnitude of the field-induced increase in the fluorescence lifetime of NADH has a tendency to increase with a decreasing pulse width. It is also found that apoptosis can be induced only in cancer cells using a suitable nsPEF, showing a possibility that ultrashort pulsed electric field is applicable for drug-free cancer therapy.

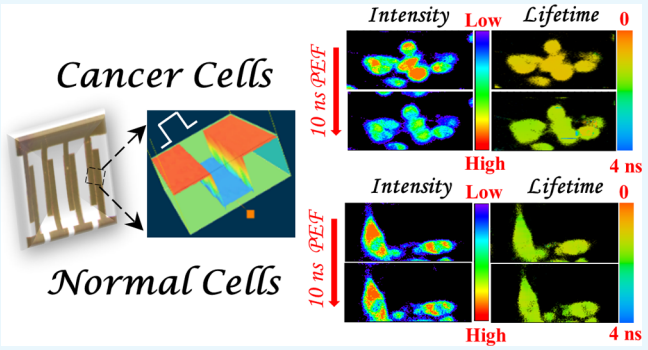

INTRODUCTION

Cancer research is of great interest in many scientific disciplines, not only in biological and medical sciences but also in chemical and spectroscopic sciences. Research in the latter has rapidly advanced the understanding of biological insights and its translation into better cancer detection and therapy.[1−5] The metabolic differences between normal and cancer cells result in different circumstances of coenzymes, which are strongly involved in cell metabolism. Nicotinamide adenine dinucleotide (NADH) is one of the important coenzymes in cellular respiration, and both the intensity and lifetime of autofluorescence of NADH in cells is markedly dependent on cellular environments.[6−13] NADH emits fluorescence at around 450 nm, and the autofluorescence of NADH is widely used to examine intracellular environments.[12] Intracellular differences between the cancer and normal cells may also be proposed to be distinguished by NADH autofluorescence.[13] In the present study, differences in the intracellular environment between normal (healthy) and cancer cells were examined using fluorescence lifetime microscopy (FLIM) of NADH before and after application of a nanosecond pulsed electric field (nsPEF). FLIM is one of the more powerful methods to perform quantitative measurements of the intracellular environment because the fluorescence lifetime is an intrinsic parameter that is independent of absorption intensity, excitation light intensity, or photobleaching.[14−20] The FLIM of autofluorescence is therefore a highly reliable and less invasive method without dye staining.[9−13,16]

The electric-field effect on the dynamics and function of biological systems may depend on the cell membrane capacitance and on the pulse duration of the applied field, which enables selective applications of pulsed electric field in specific organelles and specific living cells.[21−23] If a pulse shorter than the charging time of the outer membrane is applied to living systems, the pulsed electric field may induce changes in subcellular organelles, signal proteins, and biochemical processes, without affecting the outer plasma membrane and organelles. For example, apoptosis is induced by the application of nsPEF, with a pulse width of 10−50 ns and a field strength of 40 or 45 kV cm^{-1} in HeLa cells.[24,25] In the present study, on the basis of the pulse-height dependence and pulse-width dependence of the field-induced change in the fluorescence lifetime, it is shown that apoptosis of cancer cells induced by application of pulsed electric fields is considerably more effective than that of normal cells, suggesting that ultrashort pulsed electric field is applicable for cancer therapy.

Received: March 15, 2017
Accepted: June 9, 2017
Published: June 22, 2017

DOI: 10.1021/acsomega.7b00315
ACS Omega 2017, 2, 2916−2924

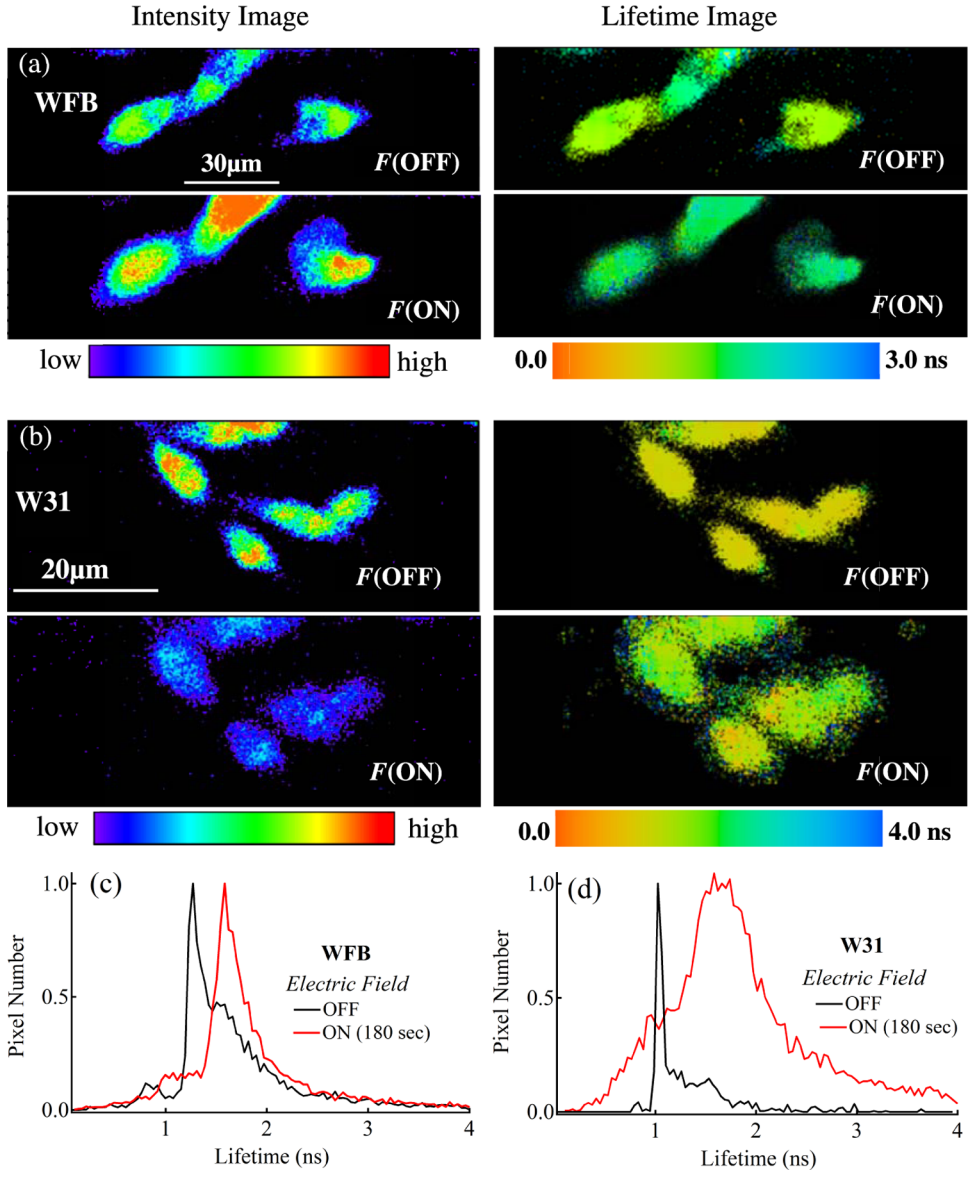

Figure 1. Autofluorescence intensity images (left) and lifetime images (right) of NADH before and after the application of an electric field for 3 min, with a 10 ns pulse width, a field strength of 45 kV cm^{-1}, and 1 kHz frequency, shown by F(OFF) and F(ON), respectively, in normal cells (WFB) (a) and in cancer cells (W31) (b). The corresponding histograms of the fluorescence lifetimes are shown in (c) and (d).

RESULTS AND DISCUSSION

When a pulsed electric field (F) is applied to a spherical cell, the voltage increase, that is, ΔV_c, across the cell membrane as a function of time, t, is given as follows[26]

$$\Delta V_c = fFr \cos\theta\left(1 - \exp\left(\frac{-t}{\tau_c}\right)\right) \quad (1)$$

Here, f is the internal field factor, r is the radius of the spherical cell, τ_c is the charging time constant of the outer cell membrane, θ is the angle between the cell radius vector and electric field. Here, the effect of the substructure of the potential distribution is assumed to be negligible. When the pulse width of the applied electric field is large enough in comparison with τ_c, the voltage across the membrane becomes very large, resulting in a breakdown of the cell membrane and production of the pore on the cell surface. When the pulse width of the applied electric field is small enough, on the other hand, the voltage across the membrane is negligible, resulting in a deep penetration of the applied electric field into the intracellular organs. In a single-shell model, τ_c is roughly estimated to be 150 ns, assuming a spherical cell having a radius of 10 μm, internal and external resistivity of 100 Ω cm, membrane capacitance of 1 μF cm^{-2}, and the volume fraction of the cell in suspension as much smaller than 1.[25] If the nsPEF, whose pulse width is less than 50 ns, is applied to cells, therefore, the applied field is expected to be penetrated into the cell before the charging of the cell membrane and intracellular function may be affected.

The effects of nsPEF on lifetime and intensity of the autofluorescence of NADH were examined in cancer and normal cells, that is, Wistar-King-Aptekman rat fetus fibroblast (WFB) cells and W31 cells, which are the malignant transformed cells from WFB. The cells were incubated between the microelectrodes used for application of nsPEF (Figure S1 in Supporting Information (SI)), which were introduced in the

DOI: 10.1021/acsomega.7b00315
ACS Omega 2017, 2, 2916−2924

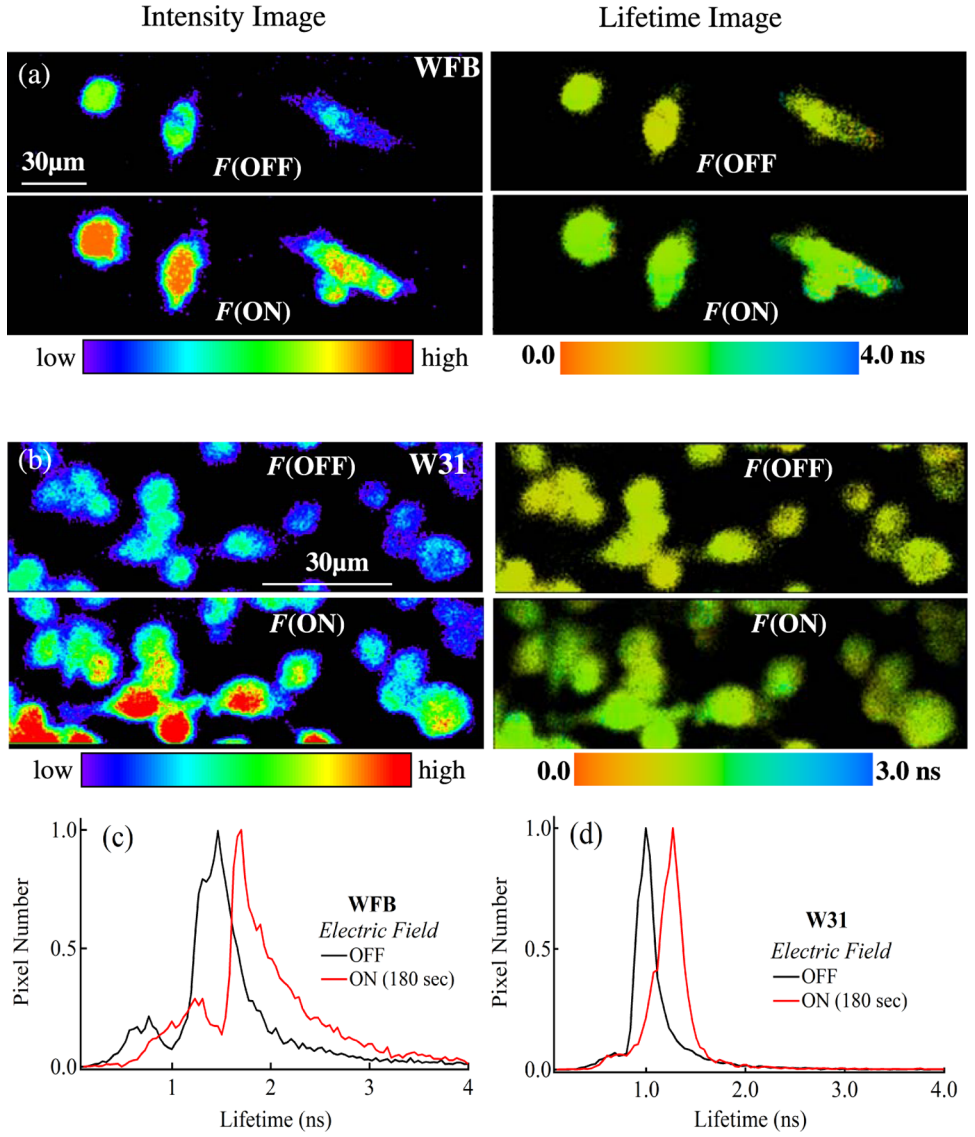

Figure 2. Autofluorescence intensity images (left) and lifetime images (right) of NADH before and after application of an electric field for 3 min, with a 30 ns pulse width, a field strength of 45 kV cm^{-1}, and 1 kHz frequency, shown by *F*(OFF) and *F*(ON), respectively, in WFB (a) and in W31 cells (b). The corresponding histograms of the fluorescence lifetimes obtained from the lifetime images are shown in (c) and (d).

inverted confocal microscope. The results obtained, with a field strength of 45 kV cm^{-1}, a pulse width of 10 ns, a frequency of 1 kHz, and 180 s application time, are shown in Figure 1. As shown in Figure S2, the fluorescence decay profiles of NADH were fitted by assuming a multiexponential decay. The fluorescence of NADH was selectively observed at a detection wavelength of 447−470 nm, with 380 nm excitation, because we have confirmed that fluorescence spectra observed with excitation at 380 nm are assigned to the spectra of NADH both in WFB and W31 cells.[13] The pulsed electric field altered the distribution of the fluorescence intensity of NADH in each cell; the nucleus could be distinguished from other fluorescent organelles before application of the electric field because of its weak fluorescence intensity, whereas the fluorescence intensity was diffusingly distributed throughout the cell after application of the electric field. As the pulse width of the applied electric field became larger, the diffused spread of the fluorescent intensity became clearer (Figures 2 and 3). The morphology of each cell was also affected by the pulsed electric field, especially in the cancer cells; the applied electric field induced fragmentation of cancer cells, whereas a leaky blebbing was observed in normal cells. The autofluorescence lifetime of NADH was also affected by the electric fields. In both normal and cancer cells, the fluorescence lifetime of NADH was increased by application of nsPEFs (see Figures 1−3).

The total intensity of the NADH fluorescence of each cell is also affected by application of the electric fields. When the pulse width of the applied electric field was as large as 50 ns, for example, the total fluorescence intensity of each cell was largely enhanced in both normal and cancer cells (Figures 3 and 4a). As the pulse width became smaller, the magnitude of the field-induced increase in intensity became smaller in both normal and cancer cells. When the pulse width was as short as 10 ns, further, the fluorescence intensity in the cancer cells became weaker after application of nsPEF (Figure 1). Thus, normal and cancer cells showed different electric field effects from each other in the autofluorescence intensity of NADH. For 10, 30, and 50 ns pulse applications, the autofluorescence lifetime of NADH became longer, irrespective of the pulse width, when the applied field was as strong as 45 kV cm^{-1} (Figures 1−3).

DOI: 10.1021/acsomega.7b00315
ACS Omega 2017, 2, 2916−2924

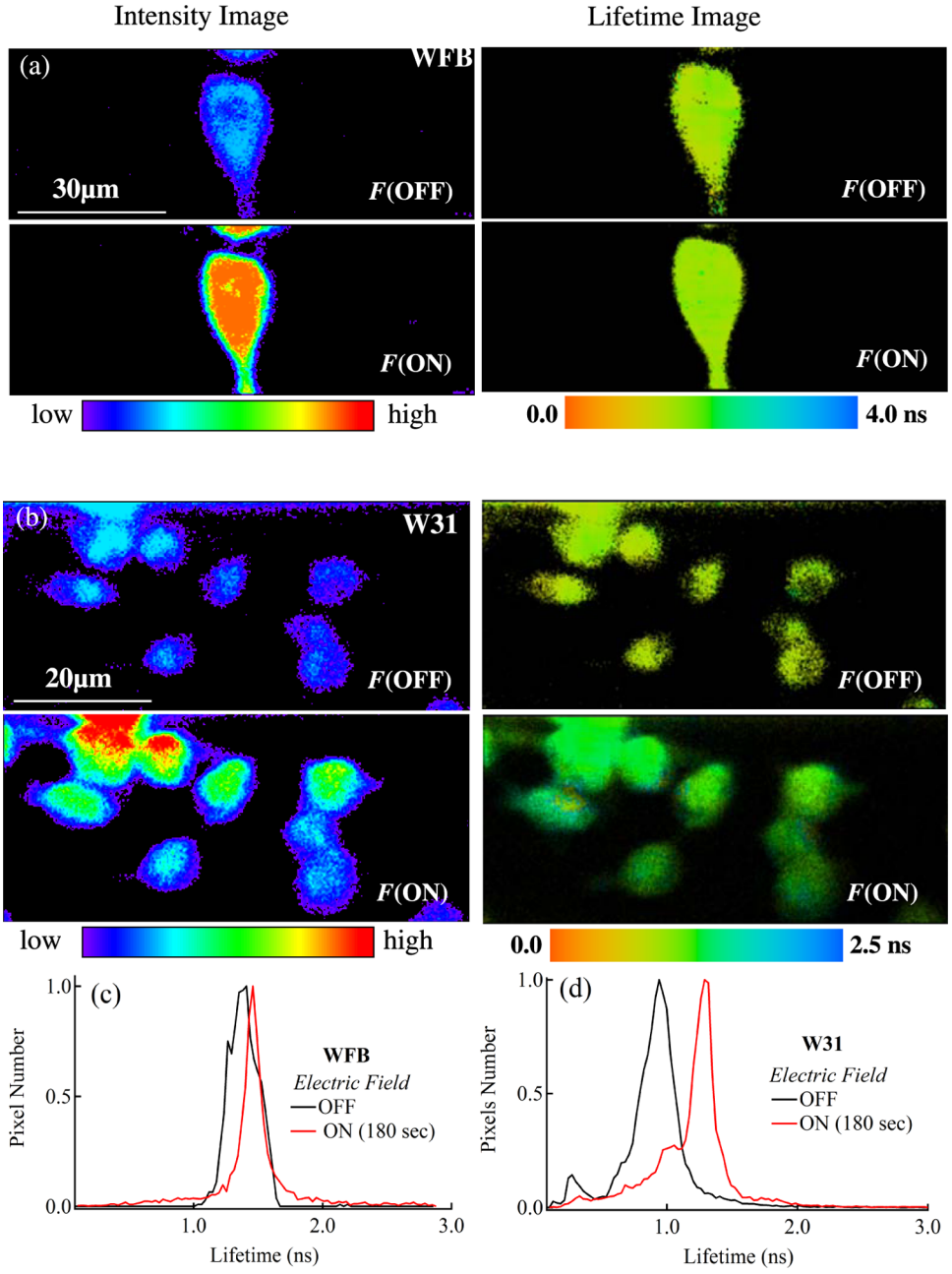

Figure 3. Autofluorescence intensity images (left) and lifetime images (right) of NADH before and after application of an electric field for 3 min, with a 50 ns pulse width, a field strength of 45 kV cm^{-1}, and 1 kHz frequency, shown by *F*(OFF) and *F*(ON), respectively, in WFB (a) and in W31 cells (b). The corresponding histograms of the fluorescence lifetimes obtained from the lifetime images are shown in (c) and (d).

Furthermore, the electric fields that had a shorter pulse width induced larger changes in the fluorescence lifetimes in both normal and cancer cells, and the ratio of the fluorescence lifetime after application of the electric field relative to that before the field application was greater in cancer cells than in normal cells at all of the pulse widths (Figure 4b). Here, it is noted that the intensity shown in Figure 4a was obtained by integrating intensities of all of the cells in each image observed before and after application of nsPEF, not for each cell. The integrated intensity of NADH fluorescence thus obtained corresponds to the intensity of one cell in Figure 3a and that of more than 10 cells in Figure 2b. To check the reproducibility, more than three experiments were done with different samples under the same experimental conditions. In relation with Figure 3a, for example, the other two experimental results of WFB before and after application of nsPEF having 50 ns pulse width and 45 kV cm^{-1} are shown in Figure S3. The fluorescence lifetime shown in Figure 4b was obtained from the peak in the histogram of the fluorescence lifetime. The error bars given in Figure 4, both in intensity and lifetime, were determined from the difference in the ratios between the results of the experiments carried out with different samples under the same experimental conditions.

In the origin of the field-induced change in fluorescence intensity, two possibilities can be considered: one is the field-induced change in the concentration of fluorescent NADH and another is the field-induced change in the fluorescence quantum yield of NADH, resulting from change in the

DOI: 10.1021/acsomega.7b00315
ACS Omega 2017, 2, 2916−2924

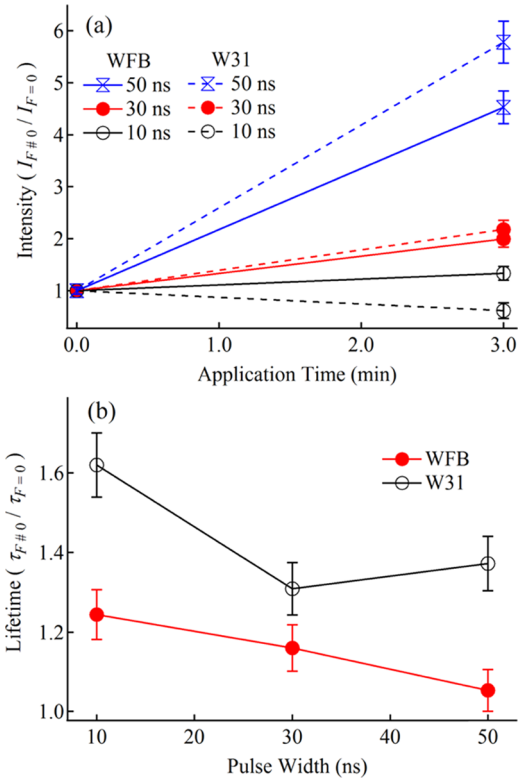

Figure 4. (a) Ratio of the fluorescence intensity of NADH obtained after application of electric field ($I_{F\neq0}$) relative to the intensity before the application ($I_{F=0}$) in normal (WFB, solid lines) and cancer cells (W31, broken lines) as a function of application time, with different pulse widths of 10, 30, and 50 ns, respectively, and 45 kV cm^{-1} field strength and 1 kHz frequency. (b) The ratio of the fluorescence lifetime of NADH after application of the electric field ($\tau_{F\neq0}$) relative to the lifetime before application ($\tau_{F=0}$), as a function of the pulse width of the applied electric field.

nonradiative decay rate of the fluorescent NADH. In every case having a pulse width of 10−50 ns, $\tau_{(F\neq0)}/\tau_{(F=0)} > 1.0$ (see Figures 1−3 and 4b), that is, the fluorescence lifetime becomes longer in the presence of the electric field, indicating that nonradiative decay at the emitting state of NADH autofluorescence becomes slower with the application of nsPEF. In other words, the fluorescence quantum yield is considered to increase in the presence of nsPEF. If the concentration of NADH is independent of the application of nsPEF, the fluorescence intensity of NADH should be increased by application of nsPEF. The decrease in the nonradiative decay rate may indicate that the protein binding of NADH becomes stronger. As shown in Figure 4, fluorescence intensity becomes higher by a factor of more than 4 both in WFB and in W31, with a pulse width of 50 ns, whereas the increase in the lifetime is less than twice in both cases. These results show that the field-induced increase in the intensity cannot be explained only by increase in the fluorescence quantum yield. Then, there is no doubt that the field-induced increase in the fluorescence intensity, with a pulse width of 50 ns, mainly results from the field-induced increase in the number of fluorophores, that is, the concentration of the emitting species of NADH is increased by the application of nsPEF. When the pulse width is as short as 10 ns, field-induced decrease in fluorescence intensity is observed in W31 (see Figures 1b and 4a, indicating that the concentration of NADH in W31 is decreased by application of nsPEF). Thus, the field-induced change in concentration of NADH depends on the pulse width of the applied nsPEF although the fluorescence lifetime of NADH becomes longer by application of the electric field irrespective of the pulse width of the applied nsPEF.

The observed pulse-width dependence of the electric field effect on the intensity and lifetime of NADH fluorescence in these normal and cancer cells is the same as the one observed in HeLa cells,[25] implying that these field effects are common in live cells. In HeLa cells, it was suggested that the so called mitochondrial permeability transition pore complex, which may induce apoptosis, is generated by the application of nsPEF, which has a pulse width as large as 50 ns. When the pulse width is as short as 10 ns, on the other hand, mitochondria outer-membrane permeabilization may be induced by nsPEF, and apoptotic factors such as cytochrome *c* and an apoptosis-inducing factor may be released into the cytosol. Thus, two mechanisms may be considered for the field-induced apoptosis, depending on the pulse width of the applied nsPEF, as suggested in the case of HeLa cells.

The electric field effect on the fluorescence lifetime of NADH may be evidence of the occurrence of apoptosis and/or necrosis. In a previous study, no major changes were observed in the autofluorescence of NADH under H_2O_2-induced necrosis in both the HeLa and 143B cells.[27] On the other hand, an increase in the NADH autofluorescence lifetime was observed during staurosporine (STS)-induced and *N*-methyl-*N*-nitro-*N*-nitrosoguanidine-induced apoptosis in the HeLa cells.[27,28] Then, we examined the relationship between the autofluorescence lifetime of NADH and apoptosis in both WFB and W31 cells using a 1 μM concentration of STS. The induction of STS is known to release cytochrome *c* from mitochondria and activate caspase-3,[29] which is one of the caspase groups that are executioners of apoptosis. It was found that the autofluorescence lifetime of NADH increased after the addition of 1 μM STS in both normal and cancer cells (Figure S4). Therefore, it is concluded that application of nsPEF induces apoptosis both in normal (WFB) and cancer (W31) cells, as in the case of the HeLa cells.[24,25] Apoptosis is traditionally defined by morphological criteria, such as cell shrinkage and cell surface blebbing. In fact, some morphological changes were detected after application of nsPEF in our study in both the cell types, depending on the amplitude and pulse width of the applied electric field, as shown in Figures S5 and S6. The detection of apoptosis using the fluorescence lifetime of NADH has a great advantage of confirming apoptosis with label-free detection, and this method has been applied in our previous study regarding the nanosecond pulsed field-induced apoptosis of HeLa cells[25] and also in a recent study by another group.[30]

Electric field-induced apoptosis, which is revealed by change in the fluorescence properties of NADH, may occur via the mitochondria-mediated pathway; the pulsed electric field acts on mitochondria to cause cytochrome *c* release from the mitochondria to the cytoplasm, along with the loss of the mitochondrial membrane potential.[31,32] The released cytochrome *c*, forms an apoptosome, which activates caspase, resulting in cellular destruction events.[33,34] The increase in the fluorescence intensity during cell death, for example, with a 50 ns pulse width, has been ascribed to the field-induced increase in the number of fluorescent NADH due to the change in the redox ratio of NADH/NAD$^+$ and/or the depletion of energy metabolism in mitochondria. A monotonic decrease in NADH

DOI: 10.1021/acsomega.7b00315
ACS Omega 2017, 2, 2916−2924

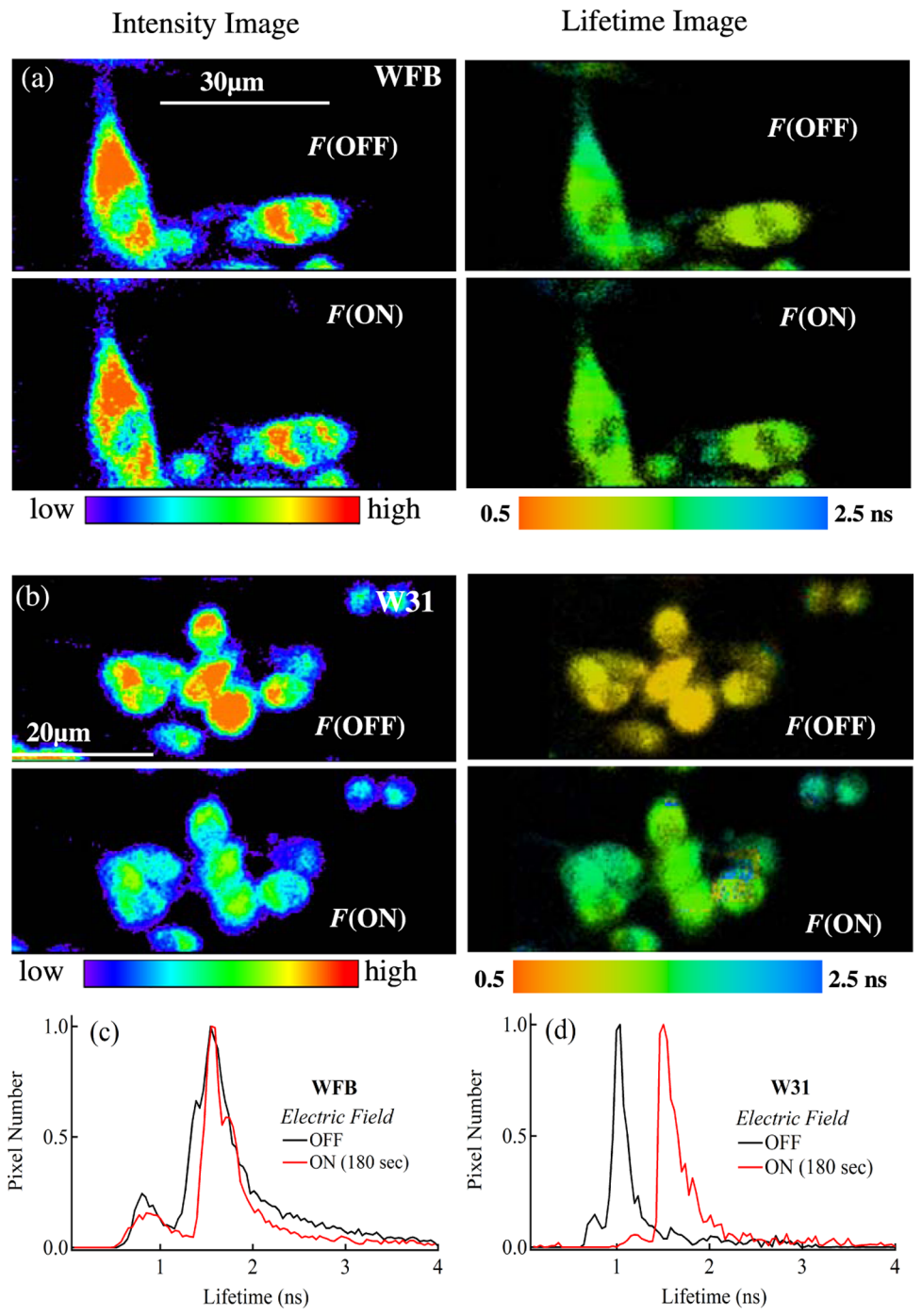

Figure 5. Autofluorescence intensity images (left) and lifetime images (right) of NADH before and after application of an electric field for 3 min, with a 10 ns pulse width, a field strength of 500 V cm^{-1}, and 1 kHz frequency, shown by *F*(OFF) and *F*(ON), respectively, in normal cells (WFB) (a) and in cancer cells (W31) (b). The corresponding histograms of the fluorescence lifetimes are shown in (c) and (d).

fluorescence intensity has previously been reported in correlation with mitochondrial membrane potential dissipation.[35] Thus, the present results of the pulse-width dependence of NADH intensity may indicate that the increase in the NADH concentration and changes in the mitochondrial transmembrane potential are involved in the apoptosis induced by application of nsPEF. Additionally, there may be a possibility that an electric field with a narrow pulse width penetrates efficiently through the outer membrane of mitochondria and directly modifies the electron transfer process of mitochondrial adenosine triphosphate production because intramolecular and intermolecular electron transfer can be affected by external electric field.[36] The pulse-width dependence of the change in NADH fluorescence intensity and lifetime and in cellular morphology is an indication of the divergent subcellular effect of pulsed electric fields on normal and cancer cells.

The intensity and lifetime images of the autofluorescence of NADH in the WFB and W31 cells were also observed before and after application of a pulsed electric field, which was as low as 500 V cm^{-1} (applied voltage of 5 V and 100 μm as a distance of electrodes), with 10 ns pulse width, 1 kHz frequency, and 180 s application time (Figure 5). The lifetime of the WFB cells

DOI: 10.1021/acsomega.7b00315
ACS Omega 2017, 2, 2916−2924

remained unchanged even after application of the pulsed fields. However, when an electric field with the same amplitude and pulse width was applied to cancer cells, the cells showed remarkable changes in morphology and in fluorescence intensity and lifetime. The change in the intensity and lifetime occurs irrespective of the location of a cell (Figure 5b), indicating that the cell death mechanism is not related to the proximity of a cell to the electrodes. Thus, the experimental results with a narrow pulse width of 10 ns showed that a magnitude as small as 500 V cm^{-1} was large enough for the applied electric field to induce apoptosis in cancer cells, whereas the healthy cells remained unaffected. To show the reproducibility of the difference of the field effect between normal and cancer cells, with a field strength of 500 V cm^{-1}, another result is shown in Figure S7. These results show that a pulsed electric field with a short pulse width has a stronger effect in cancer cells than that in healthy cells. This field-strength dependence of the applied electric field effect may work as an option to selectively kill the cancer cells, that is, an electric field with a low amplitude and short pulse width can be used to kill the cancer cells, without any serious damage to normal cells. Therefore, the application of ultrashort pulsed electric fields may become a potential technique for cancer therapy without injuring the normal cells by adjusting the applied field conditions.

The field strengths, 45 kV cm^{-1} and 500 V cm^{-1}, used in the present study were the maximum and minimum field strengths, respectively, which we could apply in the present experimental system, with stability. Further experiments are necessary to examine the detailed field-strength dependence, which will be the future problem.

CONCLUSIONS

Autofluorescence lifetime images as well as intensity images of NADH have been measured in normal and cancer cells, that is, in the WFB cells and W31 cells, which are the malignant transformed cells from WFB, before and after the application of nsPEF, having a strength of 45 kV cm^{-1}, a frequency of 1 kHz, and a pulse width of 10, 30, or 50 ns. In every case, the fluorescence lifetime of NADH becomes longer by application of nsPEF. This behavior is very similar to the change in the fluorescence lifetime of NADH in these cells observed after the addition of STS, which is a well-known apoptosis inducer. Morphological change in the cell structure is also induced by the application of pulsed electric field. These results show that apoptosis is induced in both normal and cancer cells by application of nsPEFs having a pulse width in the region of 10−50 ns. The field effect on the intensity and lifetime of NADH depends on the pulse width of the applied electric field. The magnitude of the field-induced increase in the fluorescence lifetime of NADH has a tendency to increase with decreasing pulse width, probably because the electric fields with a short pulse width can penetrate deeply into the mitochondria and initiate apoptosis more efficiently. It is also found that apoptosis can be induced only in cancer cells using a suitable nsPEF, for example, with a narrow pulse width of 10 ns and a magnitude as small as 500 V cm^{-1}, showing a possibility that an ultrashort pulsed electric field is applicable for a drug-free cancer therapy. The present experimental results of the autofluorescence intensity and lifetime in healthy and cancer cells may open a new gateway for a drug-free cancer therapy using ultrashort pulsed electric fields.

METHODS

Cell Culture. The WFB cells and W31 cells that were H-ras oncogene-transfected cells from WFB were incubated in a 5% CO_2 humidified atmosphere at 37 °C in Dulbecco's modified Eagle's medium (D5796; Sigma), supplemented with 2×10^5 U dm^{-3} penicillin G, 200 mg of streptomycin sulfate, and 10% fetal bovine serum.[13,37] The cells that were originally donated to one of the authors (L.L.) from Prof. N. Sato at Sapporo Medical University[38] were used. The cell culture medium was replaced by calcium- and magnesium-free phosphate buffered saline (PBS (−)) medium just before the measurements of the autofluorescence lifetime of NADH.

Fluorescence Lifetime Imaging. FLIM images of the endogenous fluorophores of NADH in normal cells (WFB) and cancer cells (W31) were measured using an inverted confocal microscope (C1; Nikon) equipped with an objective lens (40×, NA 0.95) and a time-correlated single photon counting system (SPC-830; Becker & Hickl GmbH).[25,39] The second harmonic output of 380 nm from a mode-locked Ti:sapphire laser (Tsunami; Spectra Physics, pulse duration of approximately 100 fs, repetition rate of 81 MHz) was used as an excitation light. Because of the low power of the excitation laser light, which was roughly estimated to be 0.03 nJ per pulse, two-photon excitation was negligible in the present experiments. The autofluorescence signal of NADH in cells was detected in the region of 447−460 nm by a microchannel-plate photomultiplier tube (R3809U; Hamamatsu). The observed decay profiles were fitted by assuming a tri-exponential decay, with a convolution of the instrumental response function, that is, the decay was assumed to be given by $\sum_i A_i \exp(-t/\tau_i)$, wherein A_i and τ_i are the preexponential factor and lifetime of the ith component, respectively, where i = 1, 2, and 3, and $\sum_i A_i\tau_i/A_i$ was obtained as the average lifetime in each pixel, the details of which were shown in refs 13 and 25. The acquisition time of the FLIM image was typically 20 min. The analysis of the FLIM data was conducted with SPC image software (Becker & Hickl GmbH).

Electrode Microchamber. A gold-coated microchannel electrode chip for in vivo observation of effects of the pulsed electric field on a single cell was constructed on a microscopic cover glass by the UV photolithography method (Figure S1 of SI). The details of the construction procedure were given in our previous papers.[24,25] Briefly, the microchamber shape was first constructed by the exposure of an SU-8 2015 negative photoresist (Micro Chem) to UV light through the mask pattern of the electrode. Then, the positive photoresist ZEP520 (ZEONREX Electronic Chemicals) was spun on the prepared microchamber and was exposed to UV light through the same mask as that used for the negative photoresist. After the chemical treatment, a layer of gold was deposited on the microchamber by helicon sputtering (MPS-4000C1/HC1; ULVAC). The substrate was baked from room temperature to 120 °C to melt ZEP520, resulting in the release of metal film from undesired areas of the substrate. The resulting electrode microchamber was immersed in acetone and cleaned by ultrasonic treatment. The distance between the electrodes was approximately 100 μm, and the final depth of the microchamber was approximately 20 μm. The WFB or W31 cells were cultured at the bottom of the electrode microchamber. A pulse generator (Avtech Electrosystems) was used to generate nsPEFs. The pulsed voltages with a width of 10, 30, or 50 ns and a strength of 450 or 5.0 V were applied, with a

DOI: 10.1021/acsomega.7b00315
ACS Omega 2017, 2, 2916−2924

load resistance of 50 Ω. The applied field strength was evaluated from the applied voltage divided by the distance between the electrodes. Therefore, the application of 450 and 5 V corresponds to a field strength of 45 kV cm^{-1} and 500 V cm^{-1}, respectively.

■ ASSOCIATED CONTENT

Supporting Information

The Supporting Information is available free of charge on the ACS Publications website at DOI: 10.1021/acsomega.7b00315.

Illustration of microelectrode, fluorescence decay profiles, fluorescence intensity and lifetime images before and after application of electric field and before and after the treatment by an apoptosis inducer (PDF)

■ AUTHOR INFORMATION

Corresponding Author

*E-mail: nohta@nctu.edu.tw.

ORCID

Nobuhiro Ohta: 0000-0003-4255-6448

Notes

The authors declare no competing financial interest.

■ ACKNOWLEDGMENTS

N.O. thanks Prof. Yuan-Pern Lee for the generous support. National Chiao Tung University and Ministry of Science and Technology (MOST) in Taiwan provided support to K.A. and N.O. This work was also supported by the Research Institute for Electronic Science, Hokkaido University, Japan.

■ REFERENCES

(1) Hanahan, D.; Weinberg, R. A. Hallmarks of Cancer: The Next Generation. *Cell* **2011**, *144*, 646−674.

(2) Ellenbroek, S. I. J.; van Rheenen, J. Imaging Hallmarks of Cancer in Living Mice. *Nat. Rev. Cancer* **2014**, *14*, 406−418.

(3) Chinen, A. B.; Guan, C. M.; Ferrer, J. R.; Barnaby, S. N.; Merkel, T. J.; Mirkin, C. A. Nanoparticle Probes for the Detection of Cancer Biomarkers, Cells, and Tissues by Fluorescence. *Chem. Rev.* **2015**, *115*, 10530−10574.

(4) Nguyen, K. T.; Zhao, Y. Engineered Hybrid Nanoparticles for On-Demand Diagnostics and Therapeutics. *Acc. Chem. Res.* **2015**, *48*, 3016−3025.

(5) Wang, W.; Zhao, J.; Short, M.; Zeng, H. Real-Time in Vivo Cancer Diagnosis Using Raman Spectroscopy. *J. Biophotonics* **2015**, *8*, 527−545.

(6) Huang, S.; Heikal, A. A.; Webb, W. W. Two-Photon Fluorescence Spectroscopy and Microscopy of NAD(P)H and Flavoprotein. *Biophys. J.* **2002**, *82*, 2811−2825.

(7) Kasischke, K. A.; Vishwasrao, H. D.; Fisher, P. J.; Zipfel, W. R.; Webb, W. W. Neural Activity Triggers Neuronal Oxidative Metabolism Followed by Astrocytic Glycolysis. *Science* **2004**, *305*, 99−103.

(8) Skala, M. C.; Riching, K. M.; Gendron-Fitzpatrick, A.; Eickhoff, J.; Eliceiri, K. W.; White, J. G.; Ramanujam, N. In Vivo Multiphoton Microscopy of NADH and FAD Redox States, Fluorescence Lifetimes, and Cellular Morphology in Precancerous Epithelia. *Proc. Natl. Acad. Sci. U.S.A.* **2007**, *104*, 19494−19499.

(9) Ghukasyan, V. V.; Kao, F.-J. Monitoring Cellular Metabolism with Fluorescence Lifetime of Reduced Nicotinamide Adenine Dinucleotide. *J. Phys. Chem. C* **2009**, *113*, 11532−11540.

(10) Chorvat, D., Jr.; Chorvatova, A. Multi-Wavelength Fluorescence Lifetime Spectroscopy: A New Approach to the Study of Endogenous Fluorescence in Living Cells and Tissues. *Laser Phys. Lett.* **2009**, *6*, 175−193.

(11) Yu, Q.; Heikal, A. A. Two-Photon Autofluorescence Dynamics Imaging Reveals Sensitivity of Intracellular NADH Concentration and Conformation to Cell Physiology at the Single-Cell Level. *J. Photochem. Photobiol. B* **2009**, *95*, 46−57.

(12) Ohta, N.; Nakabayashi, T. Intracellular Autofluorescent Species: Structure, Spectroscopy, and Photophysics. In *Natural Biomarkers for Cellular Metabolism, Biology, Techniques, and Applications*; Ghukasyan, V. V., Heikal, A. A., Eds.; CRC Press: Boca Raton, 2014; pp 41−64.

(13) Awasthi, K.; Moriya, D.; Nakabayashi, T.; Li, L.; Ohta, N. Sensitive Detection of Intracellular Environment of Normal and Cancer Cells by Autofluorescence Lifetime Imaging. *J. Photochem. Photobiol. B* **2016**, *165*, 256−265.

(14) Wallrabe, H.; Periasamy, A. Imaging Protein Molecules Using FRET and FLIM Microscopy. *Curr. Opin. Biotechnol.* **2005**, *16*, 19−27.

(15) Levitt, J. A.; Matthews, D. R.; Ameer-Beg, S. M.; Suhling, K. Fluorescence Lifetime and Polarization-Resolved Imaging in Cell Biology. *Curr. Opin. Biotechnol.* **2009**, *20*, 28−36.

(16) Berezin, M. Y.; Achilefu, S. Fluorescence Lifetime Measurements and Biological Imaging. *Chem. Rev.* **2010**, *110*, 2641−2684.

(17) Borst, J. W.; Visser, A. J. W. G. Fluorescence Lifetime Imaging Microscopy in Life Sciences. *Meas. Sci. Technol.* **2010**, *21*, No. 102002.

(18) Becker, W. Fluorescence Lifetime Imaging-Techniques and Applications. *J. Microsc.* **2012**, *247*, 119−136.

(19) Nakabayashi, T.; Wang, H.-P.; Kinjo, M.; Ohta, N. Application of Fluorescence Lifetime Imaging of Enhanced Green Fluorescent Protein to Intracellular pH Measurements. *Photochem. Photobiol. Sci.* **2008**, *7*, 668−670.

(20) Lakowicz, J. R.; Szmacinski, H.; Nowaczyk, K.; Johnson, M. L. Fluorescence Lifetime Imaging of Free and Protein-Bound NADH. *Proc. Natl. Acad. Sci. U.S.A.* **1992**, *89*, 1271−1275.

(21) Schoenbach, K. H. Bioelectric Effect of Intense Nanosecond Pulses. In *Advanced Electroporation Techniques in Biology and Medicine*; Pakhomov, A. G., Miklavcic, D., Markov, M. S., Eds.; CRC Press: Boca Raton, 2010; pp 19−49.

(22) Zhang, K.; Guo, J.; Ge, Z.; Zhang, J. Nanosecond Pulsed Electric Fields (nsPEFs) Regulate Phenotypes of Chondrocytes through Wnt/β-catenin Signaling Pathway. *Sci. Rep.* **2014**, *4*, No. 5836.

(23) Wei, K.; Li, W.; Gao, S.; Ji, B.; Zang, Y.; Su, B.; Wang, K.; Yao, M.; Zhang, J.; Wang, J. Inactivation of Ricin Toxin by Nanosecond Pulsed Electric Fields Including Evidences from Cell and Animal Toxicity. *Sci. Rep.* **2016**, *6*, No. 18781.

(24) Awasthi, K.; Nakabayashi, T.; Ohta, N. Application of Nanosecond Pulsed Electric Fields into HeLa Cells Expressing Enhanced Green Fluorescent Protein and Fluorescence Lifetime Microscopy. *J. Phys. Chem. B* **2012**, *116*, 11159−11165.

(25) Awasthi, K.; Nakabayashi, T.; Ohta, N. Effects of Nanosecond Pulsed Electric Fields on the Intracellular Function of HeLa Cells as Revealed by NADH Autofluorescence Microscopy. *ACS Omega* **2016**, *1*, 396−406.

(26) Schoenbach, K. H.; Joshi, R. P.; Kolb, J. F.; Chen, N.; Stacey, M.; Blackmore, P. F.; Buescher, E. S.; Beebe, S. J. Ultrashort Electrical Pulses Open a New Gateway Into Biological Cells. *Proc. IEEE* **2004**, *92*, 1122−1137.

(27) Wang, H.-W.; Gukassyan, V.; Chen, C.-T.; Wei, Y.-H.; Guo, H.-W.; Yu, J.-S.; Kao, F.-J. Differentiation of Apoptosis from Necrosis by Dynamic Changes of Reduced Nicotinamide Adenine Dinucleotide Fluorescence Lifetime in Live Cells. *J. Biomed. Opt.* **2008**, *13*, No. 054011.

(28) Wang, H.-W. NAD(P)H and FAD as Biomarkers for Programmed Cell Death. In *Natural Biomarkers for Cellular Metabolism, Biology, Techniques, and Applications*; Ghukasyan, V. V., Heikal, A. A., Eds.; CRC Press: Boca Raton, 2014; pp 215−223.

(29) Maeno, E.; Shimizu, T.; Okada, Y. Normotonic Cell Shrinkage Induces Apoptosis under Extracellular Low Cl Conditions in Human Lymphoid and Epithelial Cells. *Acta Physiol.* **2006**, *187*, 217−222.

(30) Bower, A. J.; Marjanovic, M.; Zhao, Y.; Li, J.; Chaney, E. J.; Boppart, S. A. Label-Free in Vivo Cellular-Level Detection and Imaging of Apoptosis. *J. Biophotonics* **2017**, *10*, 143−150.

DOI: 10.1021/acsomega.7b00315
ACS Omega 2017, 2, 2916−2924

(31) Kluck, R. M.; Bossy-Wetzel, E.; Green, D. R.; Newmeyer, D. D. The Release of Cytochrome *c* from Mitochondria: A Primary Site for Bcl-2 Regulation of Apoptosis. *Science* **1997**, *275*, 1132−1136.
(32) Green, D. R.; Reed, J. C. Mitochondria and Apoptosis. *Science* **1998**, *281*, 1309−1312.
(33) Blankenberg, F. G. In Vivo Imaging of Apoptosis. *Cancer Biol. Ther.* **2008**, *7*, 1525−1532.
(34) Schon, E. A.; Manfredi, G. Neuronal Degeneration and Mitochondrial Dysfunction. *J. Clin. Invest.* **2003**, *111*, 303−312.
(35) Petit, P. X.; Gendron, M.-C.; Schrantz, N.; Metivier, D.; Kroemer, G.; Maciorowska, Z.; Sureau, F.; Koester, S. Oxidation of Pyridine Nucleotides during Fas- and Ceramide-Induced Apoptosis in Jurkat Cells: Correlation with Changes in Mitochondria, Glutathione Depletion, Intracellular Acidification and Caspase 3 Activation. *Biochem. J.* **2001**, *353*, 357−367.
(36) Ohta, N. Electric Field Effects on Photochemical Dynamics in Solid Films. *Bull. Chem. Soc. Jpn.* **2002**, *75*, 1637−1655.
(37) Shirogane, R.; Sasabe, H.; Sato, N.; Li, L. Discrimination of Normal and Cancer Cells from Autofluorescence Spectra by Laser Excitation. *Mol. Cryst. Liq. Cryst.* **2010**, *519*, 163.
(38) Yagihashi, A.; Sato, N.; Torigoe, T.; Okubo, M.; Konno, A.; Takahashi, N.; Yamashita, T.; Fujinaga, K.; Kuzumaki, N.; Kikuchi, K. Identification of the Transformation-Associated Cell Surface Antigen Expressed on the Rat Fetus-Derived Fibroblast. *Cancer Res.* **1988**, *48*, 2798−2804.
(39) Ogikubo, S.; Nakabayashi, T.; Adachi, T.; Islam, Md. S.; Yoshizawa, T.; Kinjo, M.; Ohta, N. Intracellular pH Sensing Using Autofluorescence Lifetime Microscopy. *J. Phys. Chem. B* **2011**, *115*, 10385−10390.

DOI: 10.1021/acsomega.7b00315
ACS Omega 2017, 2, 2916−2924